The Niemann-Pick type C2 protein loads isoglobotrihexosylceramide onto CD1d molecules and contributes to the thymic selection of NKT cells

Nicolas Schrantz,[1] Yuval Sagiv,[2] Yang Liu,[3] Paul B. Savage,[3] Albert Bendelac,[2] and Luc Teyton[1]

[1]Department of Immunology, The Scripps Research Institute, La Jolla, CA 92037
[2]Committee on Immunology, University of Chicago, Chicago, IL 60637
[3]Department of Chemistry, Brigham Young University, Provo, UT 84602

The Niemann-Pick type C2 (NPC2) protein is a small, soluble, lysosomal protein important for cholesterol and sphingolipid transport in the lysosome. The immunological phenotype of NPC2-deficient mice was limited to an impaired thymic selection of Vα14 natural killer T cells (NKT cells) and a subsequent reduction of NKT cells in the periphery. The remaining NKT cells failed to produce measurable quantities of interferon-γ in vivo and in vitro after activation with α-galactosylceramide. In addition, thymocytes and splenocytes from NPC2-deficient mice were poor presenters of endogenous and exogenous lipids to CD1d-restricted Vα14 hybridoma cells.

Importantly, we determined that similar to saposins, recombinant NPC2 was able to unload lipids from and load lipids into CD1d. This transfer activity was associated with a dimeric form of NPC2, suggesting a unique mechanism of glycosphingolipid transfer by NPC2. Similar to saposin B, NPC2 dimers were able to load isoglobotrihexosylceramide (iGb3), the natural selecting ligand of NKT cells in the thymus, into CD1d. These observations strongly suggested that the phenotype observed in NPC2-deficient animals was directly linked to the efficiency of the loading of iGb3 into CD1d molecules expressed by thymocytes. This conclusion was supported by the rescue of endogenous and exogenous iGb3 presentation by recombinant NPC2. Thus, the loading of endogenous and exogenous lipids and glycolipids onto CD1d is dependent on various small, soluble lipid transfer proteins present in the lysosome.

CORRESPONDENCE
Luc Teyton:
lteyton@scripps.edu

Abbreviations used: DHE, dehydroergosterol; GM2a, GM2 activator; iGb3, isoglobotrihexosylceramide; LacCer, lactosylceramide; LTP, lipid transfer protein; NKT cell, NK T cell; NPC1, Niemann-Pick type C1; NPC2, Niemann-Pick type C2; NTA, nitrilotriacetic acid.

CD1 molecules are nonpolymorphic MHC class I–like proteins that associate with β2-microglobulin and present lipids and glycolipids to the immune system. Mammalian CD1 proteins segregate into group I (CD1a, CD1b, and CD1c) and group II (CD1d) based on sequence homologies (1, 2). Mice express CD1d only. Its distribution is limited to macrophages, monocytes, B cells, DCs, and cortical thymocytes (3, 4). CD1d is the restriction element for two groups of T cells that recognize lipids. The first group is indistinguishable from classic T cells and has been identified in humans for lipids as diverse as mycobacterial mycolic acids and endogenous sulfatide (5–7). The second group represents a unique, small population of T cells called NK T cells (NKT cells) that is essential for the regulation of immune responses (8). NKT cells represent an ideal system for the study of lipid antigens because agonist ligands such as α-galactosyl and α-glucuronosyl ceramides have been identified, and the main thymic selecting ceramide, isoglobotrihexosylceramide (iGb3), is known (9, 10). NKT cells express a unique TCR-α chain (Vα14-Jα18 in the mouse and Vα24-Jα18 in the human) paired with a restricted set of Vβ segments (Vβ8, Vβ7, and Vβ2 in the mouse and Vβ11 in the human; references 11, 12).

Unlike conventional αβ T cells, NKT cells are selected by $CD4^+CD8^+$ cortical thymocytes, not by epithelial cells (12, 13). This selection process requires the intracellular trafficking of CD1d to late endosomal and lysosomal

The online version of this article contains supplemental material.

compartments (14). The main endogenous self-glycolipid that, once bound to CD1d, selects canonical Vα14 NKT cells was recently identified as iGb3, a sphingolipid that is produced in small quantities by iGb3 synthases and mainly by the degradation of isoglobotetrahexosylceramide by glycosidase β–hexosaminidase b, as illustrated by the absence of Vα14 NKT cells in hexosaminidase b–deficient mice (10, 15). We have shown in vitro and in vivo that iGb3 could not load CD1d spontaneously but rather required the assistance of lipid transfer proteins (LTPs) such as saposin (10). The number of known lysosomal LTPs is limited, and their main members are saposins A–D, GM2 activator (GM2a), and Niemann-Pick type C2 (NPC2; references 16–18). The overlap of transfer activity between these different molecules is rather large, as they all bind similar glycolipids such as gangliosides (19, 20). However, each has its own specificity and profile, as exemplified by the capacity of saposin B and GM2a to transfer αGalCer to CD1d and the inability or low activity of any of the other saposins to do so (reference 21; unpublished data). This situation suggested to us that in the lysosome, the repertoire of lipid bound to CD1 could be the result of glycolipid loading by multiple LTPs.

NPC2 is a 22-kD soluble lysosomal glycoprotein that is expressed ubiquitously and secreted as a mannose-6-phosphate–tagged protein (22, 23). NPC2 is the only small LTP that has been identified consistently in the lysosomal proteome next to saposin (17, 18). NPC2 binds and transfers cholesterol, but its precise function is still undefined (24). Its deficiency leads to a small (~5%) complementation group of Niemann-Pick disease, which is clinically indistinguishable from Niemann-Pick type C1 (NPC1) deficiency (25, 26). The identical phenotype is rather surprising, as evidence has accumulated to demonstrate that there are no physical relationships between the two molecules (17, 27, 28).

However, immunological phenotypes appear to be sufficiently subtle to attribute specific functions to both NPC1 and NPC2 and separate the two complementation groups. We have recently reported that NPC1-deficient mice lacked Vα14 NKT cells and that this phenotype was linked to an abnormal trafficking of sphingolipid antigens to the lysosome, which is secondary to a late endosomal block/accumulation (29). In the present study, we investigated the impact of a deficiency in NPC2 production with respect to Vα14 NKT development and functions. As for NPC1-deficient mice, the NPC2-deficient animal exhibited an important reduction of Vα14 NKT cell numbers, and the presentation of endogenous and exogenous lipid antigens by NPC2-deficient thymocytes and splenocytes was substantially reduced. However, in contrast to NPC1 deficiency, NPC2 absence did not lead to a noticeable late endosomal block of lipid trafficking to the lysosome. Antigen presentation deficiency was reversed by the addition of exogenous recombinant NPC2. In vitro, NPC2 was able to load iGb3 into CD1d molecules, and only dimers of the molecule were able to transfer iGb3 and other glycolipids to CD1, arguing that cholesterol and sphingolipid transfers by NPC2 might operate differently. Our data indicate that NPC2 participates in the loading of endogenous lipids into CD1d and in the selection of NKT cells. Therefore, as suggested in this study, multiple lysosomal LTPs can operate to establish the repertoire of lipids to be presented to the immune system.

RESULTS

NPC2-deficient mice exhibit a reduction of Vα14 NKT cells

Thymocytes, splenocytes, and hepatic and blood lymphocytes from 7-wk-old NPC2$^{-/-}$ or littermate control mice were stained with CD1d-αGalCer tetramers. On the BALB/c background, the proportion of tetramer-positive cells in NPC2-deficient mice was dramatically reduced in all tissues (Fig. 1 A). In the spleen and liver, the tetramer-positive cells represented 18% and 20%, respectively, of the population observed in the WT littermate control (Fig. 1 A). In the thymus, tetramer and antibody staining distinguished two subsets of NKT cells: a resident thymic population (CD1d-αGalCer tetramer^{intermediate}, CD44^{high}, CD49b^{+}) and a larger population of cells that will immigrate to the periphery (CD1d-αGalCer tetramer^{high}, CD44^{intermediate}, CD49b^{-}; Fig. S2; references 30, 31). NPC2 deficiency was accompanied by an almost complete disappearance of the CD1d-αGalCer tetramer^{high} CD44^{int} population (2% of the littermate control population) that persisted over time (Fig. 1 B), whereas the CD1d-αGalCer tetramer^{int} CD44^{high} population was reduced to 25% early on (Fig. 1 A) but accumulated intrathymically to reach normal levels at 12 wk (Fig. 1 B). The Vα14 NKT cell selection defect was specific for Vα14 NKT cells because the thymus and the spleen of NPC2-deficient mice exhibited normal numbers of CD4, CD8, and B cells (Fig. S1, available at http://www.jem.org/cgi/content/full/jem.20061562/DC1). Identical results were obtained from NPC2 mice bred on the mixed B6/129 background (unpublished data).

These results indicate that there is a selective decrease in the thymic selection, a normal emigration to the periphery, and a small but noticeable expansion in the periphery of Vα14 NKT cells in the absence of NPC2 protein. The progressive accumulation of the resident thymic NKT cell population was reproducible but never led to increased numbers in the periphery in any of the older animals, clearly separating the behavior of these two populations.

The remaining population of NKT cells in NPC2$^{-/-}$ animals has limited functionality

The addition of the increasing concentration of αGalCer and Galα1-2GalCer to whole spleen cells leads to an NKT cell–dependent production of IFN-γ (32, 33). As expected, NPC2$^{-/-}$ NKT cells failed to produce or induce the production (through NK stimulation; reference 34) of a detectable amount of IFN-γ with either lipid (Fig. 2 A) in this assay, as they also did in vivo after i.v. injection of 2 μg αGalCer (Fig. 2 B). In this latter instance, a very limited NKT cell expansion was noticeable 6 d after the injection of αGalCer and was comparable with the WT when expressed as fold expansion using day 0 as a reference (Fig. 2, C and D).

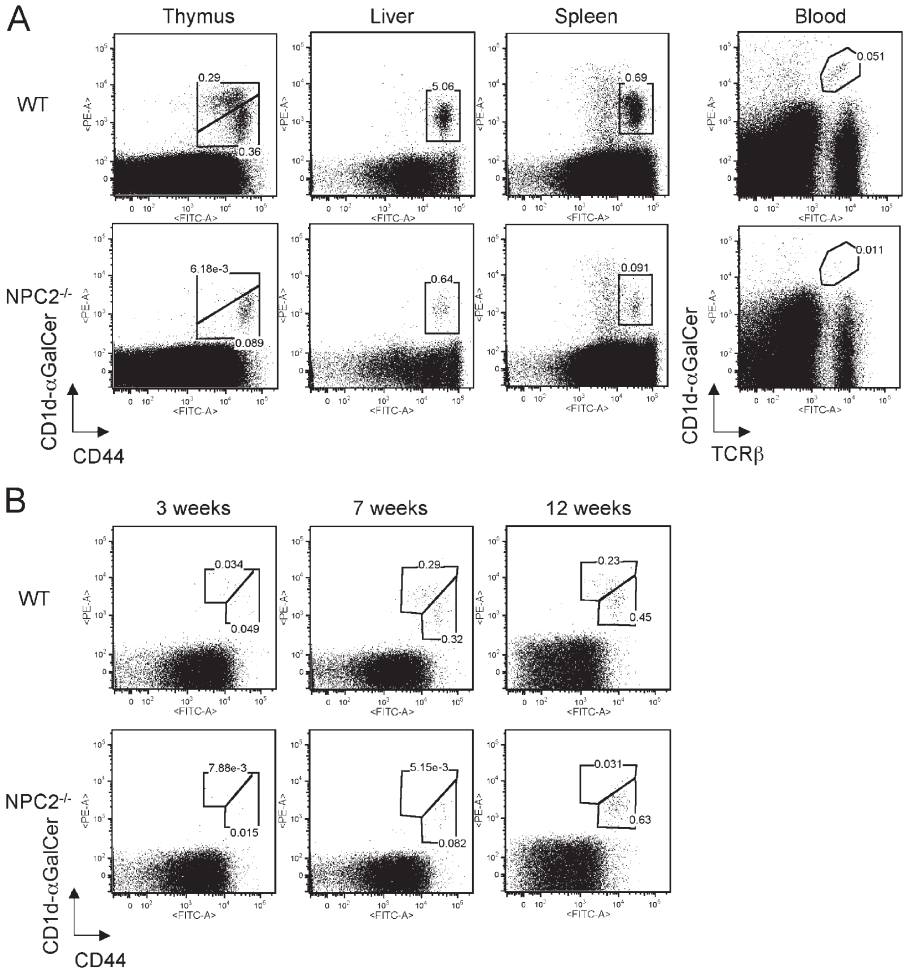

Figure 1. NPC2-deficient mice exhibit a reduction of NKT cells. (A) Vα14 NKT cells from the thymus, liver, spleen, and blood of 7-wk-old WT or NPC2-deficient ($NPC2^{-/-}$) mice were stained with CD1d-αGalCer tetramers and CD44 or TCR-β. The values in the gates indicate the absolute numbers of Vα14 NKT cells as represented by their percentages of the lymphocyte population in each organ. For the thymus, percentages are split in CD1d-αGalCer tet^{high} $CD44^{int}$ and CD1d-αGalCer tet^{int} $CD44^{high}$ cells. Percentages in the liver are percentages out of all lymphocytes. The figure is representative of two independent experiments with two animals in each group. (B) Age-related variations of NKT cell numbers. Thymocytes from 3-, 7-, and 12-wk-old WT and $NPC2^{-/-}$ mice were stained with CD1d-αGalCer tetramer and anti-CD44 antibody. Percentages of CD1d-αGalCer tet^{high} $CD44^{int}$ and CD1d-αGalCer tet^{int} $CD44^{high}$ cells are indicated in the gates. The numbers of animals analyzed per group are four, two, and five for 3 wk, 7 wk, and 12 wk, respectively. Cellularity of the thymus of $NPC2^{-/-}$ animals was normal at 3 and 7 wk and diminished by ∼30% at 12 wk of age (70.5 ± 27%) as compared with littermate controls.

This result strongly argued that the IFN-γ phenotype was linked to antigen presentation rather than to an inherent NKT cell dysfunction. A more detailed analysis of CD1d-restricted antigen presentation was undertaken in vitro.

Defective presentation of endogenous and exogenous lipid antigens by thymocytes and splenocytes from NPC2-deficient mice

The expression of CD1d molecules was normal in $NPC2^{-/-}$ animals on all cellular subsets tested, especially B cells, DCs, and thymocytes, excluding a functional knockout of CD1d and a subsequent NKT cell deficiency (Fig. S3, available at http://www.jem.org/cgi/content/full/jem.20061562/DC1). The antigen-presenting capacities of CD1d-expressing cells from deficient animals were then evaluated in vitro by using the classic DN32.D3 assay (21). This assay appreciates the expression of CD1d–iGb3 complexes in tissues by testing the capacity of primary cells such as thymocytes to stimulate the production of IL-2 from Vα14-DN32.D3 T cell hybridoma cells in the absence of exogenous antigen. Similar to the situation encountered in the absence of CD1d expression, $NPC2^{-/-}$ thymocytes were unable to stimulate DN32.D3 cells (Fig. 3 A). In contrast, the non-Vα14 NKT hybridoma TBD7 was responding identically to $NPC2^{-/-}$ and WT thymocytes, whereas the stimulation of TCB11 was reduced by ∼50% in the absence of NPC2 (Fig. 3 B). These results suggested that NPC2 deficiency specifically impaired the presentation of iGb3 by CD1d-expressing thymocytes

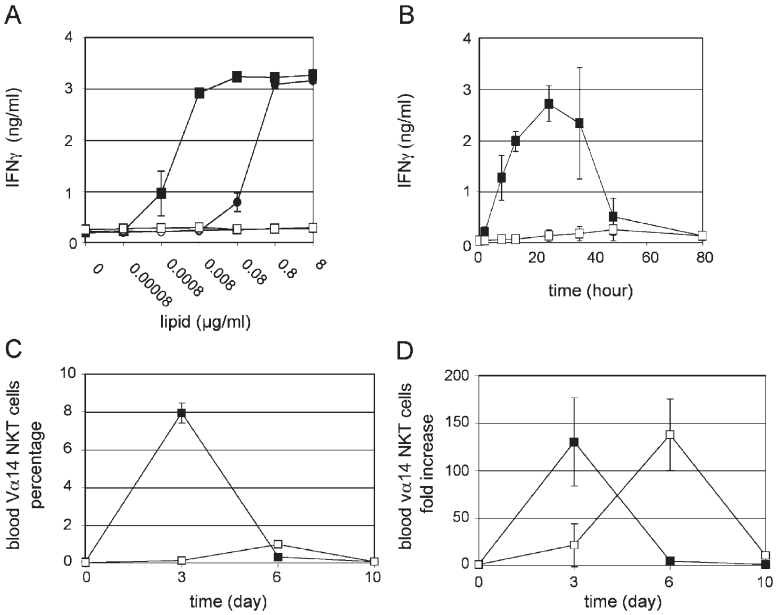

Figure 2. In vivo and in vitro functional analysis of Vα14 NKT cells. (A) Splenocytes from WT (closed symbols) or NPC2$^{-/-}$ (open symbols) were cultured with various concentrations of αGalCer (squares) or Galα1-2αGalCer (circles), and IFN-γ production in culture supernatants was measured by ELISA. (B) WT (closed squares) and NPC2$^{-/-}$ (open squares) mice were injected i.v. with 2 μg αGalCer, and the production of IFN-γ in serum was measured by ELISA. (C and D) 2 μg αGalCer was injected i.v. to WT (closed squares) and NPC2$^{-/-}$ (open squares) mice. The expansion of Vα14 NKT cells was followed in blood at different time points by staining peripheral blood lymphocytes with CD1d-αGalCer tetramer and anti-TCR-β antibody and was expressed as a percentage of lymphocytes (C) or fold increase using day 0 as a reference (D). All experiments were performed twice with two animals per group. Error bars represent SD.

but not (or only partially) the presentation of some other endogenous lipids.

The presentation of exogenous lipids was tested with αGalCer and Galα1-2GalCer, two agonists of NKT cells that are partially and completely dependent on endosomal functions, respectively (33). Stimulation of DN32.D3 by thymocytes and splenocytes from NPC2$^{-/-}$-deficient mice pulsed with αGalCer was decreased and similar to presentation by CD1d$^{-/-}$ cells, whereas the processing/presentation of Galα1-2GalCer was abolished (Fig. 3, C and D). The presentation by BM-derived DCs (BMDCs) of these same two lipids was only marginally affected (Fig. 3 E). This same phenotype of lipid presentation deficiency was found throughout the life of the NPC2$^{-/-}$ animals, as we tested mice of 3, 6, 8, 9, 10, 13, and 14 wk of age.

These results demonstrated that thymocytes and splenocytes that both express similar amounts of NPC2 in the WT (Fig. S4, available at http://www.jem.org/cgi/content/full/jem.20061562/DC1) required NPC2 for the presentation of exogenous lipids. This specific deficit argued that the absence of NPC2 did not grossly affect the CD1d/lipid-loading compartments. This functionality of the late endosomal/lysosomal compartments was confirmed by testing the presentation of MHC class II–restricted proteins such as OVA. D011.10 T cell hybridoma cells that recognize the OVA peptide 323–339 in the context of I-A$^{b/d}$ were stimulated normally by NPC2$^{-/-}$ splenocytes incubated with intact OVA (Fig. 3 F).

Trafficking of glycosphingolipids in NPC2-deficient cells

Confocal microscopic analysis of splenocytes from WT and NPC2$^{-/-}$ mice showed that CD1d was normally localized in the lysosome-associated membrane protein 1–positive late endosome/lysosome compartment of NPC2$^{-/-}$ cells (Fig. 4 A), where lipid antigens are loaded in CD1d (35). Abnormal lipid trafficking in NPC1$^{-/-}$ cells has been extensively documented (22, 36, 37). Because of cholesterol accumulation in the endosomal pathway, the transport of lactosylceramide (LacCer) to the Golgi is heavily disturbed, and fluorescent forms of αGalCer accumulate in the late endosome without ever reaching the lysosome (29). Similar studies on NPC2$^{-/-}$ cells are scarce and poorly documented. Fluorescent LacCer was fed to WT and NPC2$^{-/-}$ fibroblasts for 30 min and observed by confocal microscopy on live cells after a 90-min chase (Fig. 4 B). WT and mutant cells looked very similar, with a predominant distribution of LacCer to the Golgi apparatus (Fig. 4 B). In addition to Golgi staining, some NPC2$^{-/-}$ cells exhibited small vesicular staining reminiscent of LacCer distribution in NPC1$^{-/-}$ cells (29, 38), indicating some minor defects in endosomal transport, as would be expected.

The accumulation of cholesterol and gangliosides in cells was analyzed by flow cytometry by measuring the accumulation of Lysotracker green after a short pulse of ingestion (39). The storage of lipids in NPC2$^{-/-}$ cells was more important in splenocytes and BMDCs than in thymocytes and

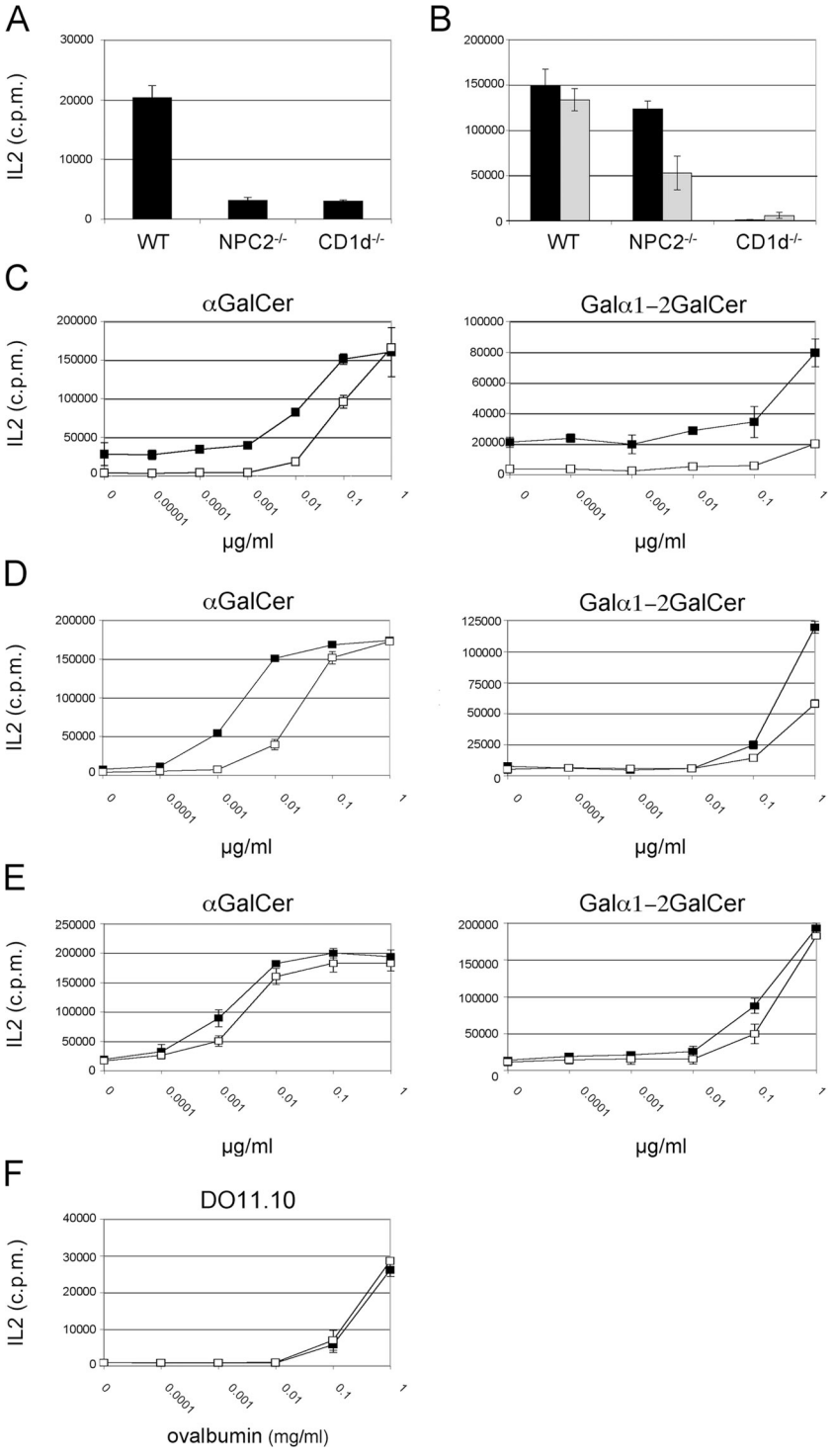

Figure 3. Defective presentation of endogenous and exogenous lipid antigens by thymocytes and splenocytes from NPC2-deficient mice. (A and B) IL-2 production by DN32.D3 hybridoma T cells (A) and non-Vα14 hybridoma TCB11 (gray) and TBD7 (black; B) cultured with thymocytes from NPC2$^{-/-}$, WT, and CD1d$^{-/-}$ mice. Data are representative of three independent experiments. (C–E) Presentation of αGalCer and Galα1-2GalCer by thymocytes (C), splenocytes (D), and BMDCs (E) from WT (closed squares) and NPC2$^{-/-}$ (open squares) mice. Data are representative of four independent experiments using mice between the ages of 6 and 9 wk. (F) Presentation of OVA protein by splenocytes from WT (closed squares) and NPC2$^{-/-}$ (open squares) mice to DO11.10 T cell hybridoma. IL-2 was measured at 24 h. Data are representative of two independent experiments. Error bars represent SD.

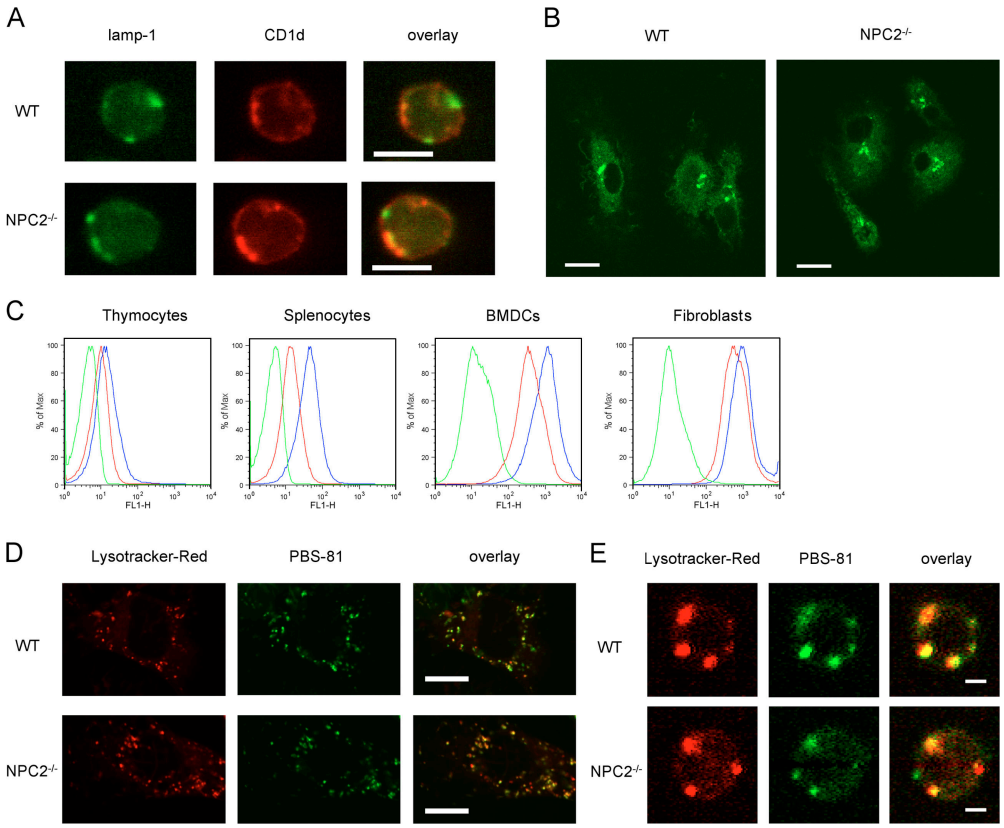

Figure 4. Trafficking of glycosphingolipids in WT and NPC2$^{-/-}$ cells. (A) Splenocytes were analyzed by confocal fluorescence microscopy for Lamp-1 (green) and CD1d (red). Individual green and red channels as well as the overlay are presented. (B) BM-derived primary fibroblasts from WT and NPC2$^{-/-}$ mice were pulsed with BODIPY-LacCer (green) and observed by confocal microscopy. (C) Evaluation of the late endosomal/lysosomal compartment size in WT and NPC2$^{-/-}$ cells. Thymocytes, splenocytes, BMDCs, and BM-derived fibroblasts from WT or NPC2$^{-/-}$ mice were stained with Lysotracker, and the fluorescence of the cells was analyzed by flow cytometry. Unstained (green), WT (red), and NPC2$^{-/-}$ (blue) profiles are presented. (D) Primary fibroblasts from WT and NPC2$^{-/-}$ mice were pulsed overnight with BODIPY-PBS-81 (green) and Lysotracker red (red) the next day and observed by confocal microscopy. Individual green and red channels as well as the overlay are presented. (E) Splenocytes were pulsed overnight with BODIPY-PBS-81 (green) and Lysotracker red (red) the next day and observed by confocal microscopy. Individual green and red channels as well as the overlay are presented. Bars (A), 5 μm; (B and D) 10 μm; (E) 2 μm.

fibroblasts when compared with the WT (Fig. 4 C). Because BMDCs and splenocytes were discordant for their presentation phenotype, we can conclude that there is no correlation between the degree of lysosomal lipid accumulation and lipid antigen presentation. The same profile of lysosomal accumulation in NPC2$^{-/-}$ cells was demonstrated for cholesterol using filipin staining (Fig. S5, available at http://www.jem.org/cgi/content/full/jem.20061562/DC1).

The overall normal transport and localization of glycosphingolipids in NPC2$^{-/-}$ cells was confirmed by examining the uptake and intracellular trafficking of a fluorescent-labeled derivative of αGalCer (BODIPY-αGalCer and PBS-81) in fibroblasts and splenocytes. Cells were pulsed for 5 h (Fig. S6, available at http://www.jem.org/cgi/content/full/jem.20061562/DC1) or overnight with PBS-81 and the lysosomal marker Lysotracker red and observed by confocal microscopy. PBS-81 accumulated in small peripheral transport vesicles and lysosomes, where they costained with the lysosomal dye. This pattern was indistinguishable between WT and NPC2-deficient cells (Fig. 4, D and E) even though the lysosomal compartment of NPC2$^{-/-}$ cells was consistently larger. Similar results were observed in BMDCs (unpublished data). These results indicated that unlike NPC1-deficient cells, NPC2-deficient cells exhibited a relatively normal uptake and trafficking of Vα14 NKT cell ligands through the endosomal compartments and to the lysosome, where they could be loaded into CD1d.

In vitro transfer of lipids to CD1d molecules by NPC2 recombinant molecules

Recombinant mouse NPC2 was produced in a fly expression system and purified by a succession of nickel–nitrilotriacetic acid (NTA) agarose, cation, and gel filtration chromatographies (40). This protocol allowed the separation of monomers and nondisulfide-linked dimers of NPC2 (Fig. 5 A). The dimeric form of mouse NPC2 was also observed after expression in HeLa cells (Fig. 5 B). Like human NPC2 protein expressed in Chinese hamster ovary cells (41), fly-expressed

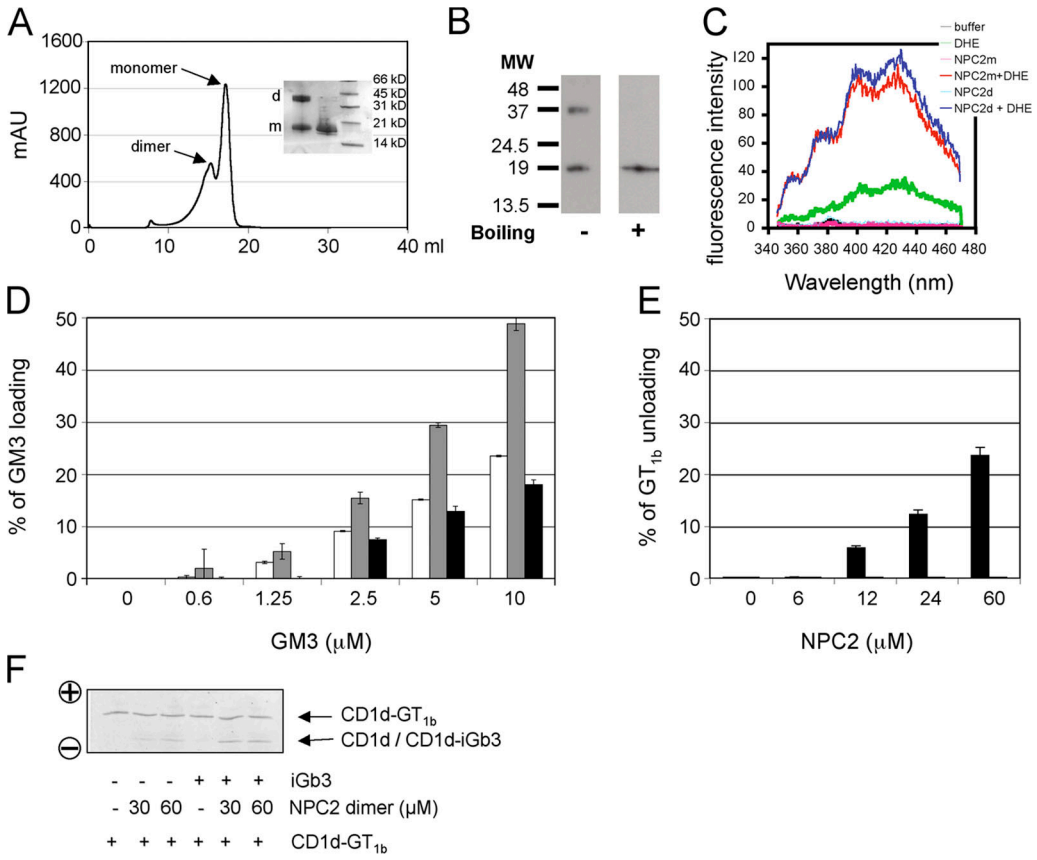

Figure 5. Oligomerization of NPC2 and in vitro loading and unloading of lipids into and from CD1d by recombinant NPC2. (A) Gel filtration profile and Coomassie blue gel of purified recombinant NPC2 protein. Fractions containing monomers and enriched in NPC2 dimers are indicated (arrows in the profile; monomers [m] and dimers [d] in the gel). (B) Expression of NPC2 in HeLa cells. Lysates from transfected HeLa cells were boiled in the presence of SDS or left untreated and analyzed by Western blotting using anti-Flag antibody. (C) Interaction of fly-expressed NPC2 protein with DHE. Fluorescent spectra of samples containing 10 μM NPC2 monomer (NPC2m) and 10 μM NPC2 dimer (NPC2d) with or without 1 μM DHE. Spectra of samples containing buffer or 1 μM DHE only are also shown. (D) 2.5 μM CD1d–GT_{1b} complexes were incubated with increasing concentrations of GM3 in the absence (white bars) or presence of 50 μM NPC2 dimers (gray bars) or 50 μM NPC2 monomers (black bars). The percentage of GM3 loading is indicated. (E) 2.5 μM CD1d–GT_{1b} complexes were incubated with increasing concentrations of NPC2 monomers (white bars) and dimers (black bars). Unloading is indicated as a percentage of GT_{1b} removal. (F) NPC2 dimers load iGb3 into CD1d. 2.5 μM CD1d–GT_{1b} complexes were incubated with increasing concentrations of NPC2 dimers in the absence or presence of 20 μM iGb3 C_{18} (iGb3). Lipid unloading and loading were visualized by native IEF. Relative positions of CD1d, CD1d–GT1b, and CD1d–iGb3 are indicated by arrows. Error bars represent SD.

mouse NPC2 protein was able to bind the fluorescent cholesterol analogue dehydroergosterol (DHE; Fig. 5 C). Interestingly, NPC2 dimers and monomers were able to bind DHE similarly (Fig. 5 C). Using a cell-free assay, we tested the ability of NPC2 dimers and monomers to transfer GM3 into CD1d (10, 21, 42). In the absence of NPC2, GM3 was poorly loaded onto CD1d. In the presence of dimers but not monomers of NPC2, the loading of GM3 into CD1d was substantially increased (Fig. 5 D). The loading of GM3 into CD1d by dimers of NPC2 was not modified by the presence of cholesterol (unpublished data). Using CD1d molecules loaded with GT_{1b}, we analyzed the ability of NPC2 to unload GT_{1b} from CD1d–GT_{1b} complexes. Again, only NPC2 dimers were able to unload GT_{1b} from CD1d (Fig. 5 E).

A similar situation was encountered when we tested the ability of NPC2 to load iGb3 into CD1d (Fig. 5 F). So far, in vitro, only saposin B had been shown to transfer iGb3 efficiently to CD1d, but recombinant NPC2 was efficient in carrying this function. This result suggests that both LTPs might act in the lysosome to load natural ligands into CD1d and select NKT cells.

Recombinant NPC2 protein enhances the presentation of ligands to Vα14 NKT cells

NPC2 accesses the lysosome after secretion through cellular uptake by the mannose-6-phosphate receptor (23). To evaluate the capacity of recombinant NPC2 to increase the uptake and loading of exogenous lipids into CD1d, WT and $NPC2^{-/-}$ splenocytes were pulsed with iGb3 in the presence

or absence of recombinant NPC2 and were used to stimulate DN32.D3 hybridoma cells. WT splenocytes presented iGb3 to DN32.D3 hybridoma with a typical dose/response curve (Fig. 6 A), whereas NPC2$^{-/-}$ splenocytes presented only the highest concentration of iGb3 (Fig. 6 B). The addition of recombinant NPC2 slightly increased the presentation of iGb3 by WT splenocytes and established normal levels of stimulation by NPC2-deficient cells (Fig. 6, A and B). This effect required CD1d, as cells from CD1d$^{-/-}$ mice could not stimulate DN32.D3 cells in the presence of recombinant NPC2 (unpublished data). The addition of recombinant GM2a, which was produced in the same expression system, did not rescue the phenotype, confirming the specificity of the effect (Fig. S7, available at http://www.jem.org/cgi/content/full/jem.20061562/DC1).

Similarly, in the absence of exogenous lipid, the addition of recombinant NPC2 to NPC2$^{-/-}$ thymocytes restored the presentation of endogenous lipids, as illustrated by the stimulation of DN32.D3 cells (Fig. 6 C). The same addition of recombinant NPC2 to WT thymocytes slightly increased their stimulatory activity (Fig. 6 C). The addition of recombinant GM2a, which was produced and purified similarly, did not rescue the phenotype or alter presentation (Fig. 6 C). Rescue of the antigen presentation phenotype of NPC2$^{-/-}$ cells by the addition of recombinant NPC2 directly demonstrates the role of NPC2 in the presentation of endogenous and exogenous lipids.

DISCUSSION

The selection of Vα14 NKT cells in the thymus is dependent on the expression of iGb3–CD1d complexes by cortical thymocytes. Presentation of the endogenous iGb3 by CD1d molecules requires the presence of iGb3 in the lysosomes and its assisted loading into CD1d by LTPs. We previously showed that the impaired production of iGb3 or the lack of saposins resulted in the severe deficiency or lack of Vα14 NKT cells (10, 21). In an attempt to find other lysosomal LTPs involved in the loading of lipid antigens into CD1d, we investigated whether NPC2 could play a role in Vα14 NKT cell selection and lipid antigen presentation.

Our study establishes that a deficiency in NPC2 profoundly affects the numbers of Vα14 NKT cells in the thymus and peripheral tissues. It is important to notice that this phenotype was observed in mice and cells that have some residual NPC2 activity (27) and that a complete knockout of expression would likely reinforce the traits that we observed. The thymic phenotype reveals two pieces of information: (a) NPC2 is required for the normal selection of Vα14 NKT cells, and (b) the resident thymic population is similarly affected, suggesting similar selecting ligands, but has the capacity to accumulate over time, indicating that it behaves differently from peripheral NKT cells. NPC2 is not involved in the egress of NKT cells from the thymus as they are found in the periphery. However, the small number of exported immature NKT cells does not lead to a normal peripheral compartment

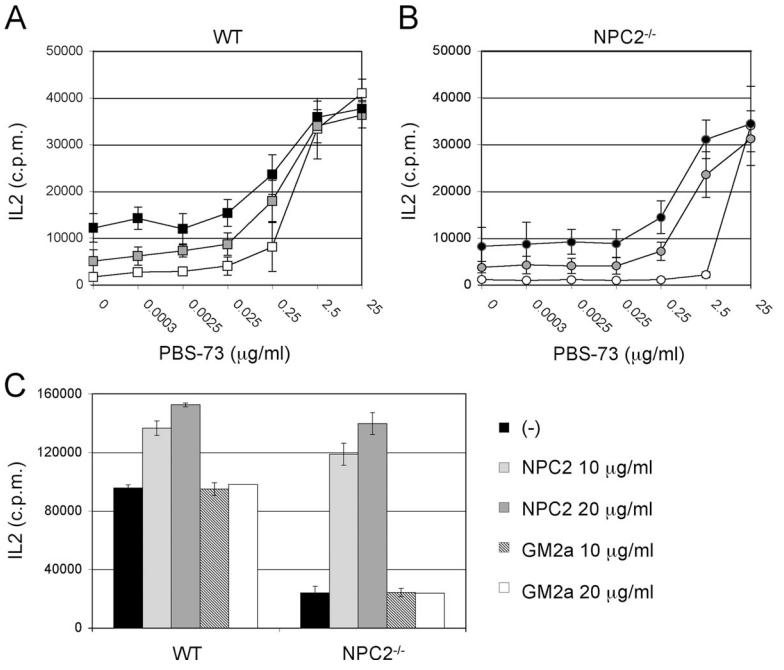

Figure 6. Exogenous NPC2 protein enhances the presentation of lipids by splenocytes and thymocytes from WT and NPC2$^{-/-}$ mice. (A and B) Splenocytes from WT (A) or NPC2$^{-/-}$ (B) mice were pulsed in the absence (white symbols) or presence of 10 (gray symbols) or 20 μg/ml (black symbols) NPC2 and increasing concentrations of iGb3 C_{18} (iGb3) for 4 h and were incubated with DN32.D3. IL-2 production was measured at 24 h. Data are representative of two independent experiments. (C) Thymocytes from WT and NPC2$^{-/-}$ mice were incubated for 24 h in the absence or presence of 10 or 20 μg/ml NPC2 or GM2a and with DN32.D3 T cells. Data are representative of two independent experiments. Error bars represent SD.

through expansion, as the deficit remains severe throughout the life of these animals.

The delay observed in the expansion of peripheral NKT cells in NPC2$^{-/-}$ animals suggests that in these mice, mainly DCs present αGalCer to Vα14 NKT cells, as it is known that the injection of αGalCer-pulsed DCs induces a delayed expansion of Vα14 NKT cells and cytokine production as compared with the injection of αGalCer alone (43). In addition, the normal degree of expansion of Vα14 NKT cells in NPC2$^{-/-}$ mice suggests that NPC2 deficiency does not affect the function of Vα14 NKT cells but only antigen presentation.

The defect of the presentation of exogenous glycosphingolipid such as αGalCer and Galα1-2αGalCer by NPC2-deficient splenocytes and thymocytes, whereas the presentation of these same lipids by BMDCs was only slightly affected, indicates that the LTP requirements for exogenous lipid uptake and presentation are different between various cell types. It also strongly suggests a model in which multiple LTPs shape the repertoire of lipid presented by CD1d molecules. This hypothesis is also supported by the profile of stimulation of non-Vα14 NKT cells by NPC2$^{-/-}$ cells. Although TCB11 stimulation was normal, TBD7 stimulation was partially affected. We have not encountered this discrepant phenotype in prosaposin-deficient animals and GM2a$^{-/-}$ mice in which both stimulations were normal (references 10, 21; unpublished data). The almost normal presentation of lipids by DCs derived from NPC2$^{-/-}$ mice also suggests that in vitro matured DCs do not faithfully represent some of the DC subsets present (for example, in the spleen). This situation will compel us to examine the presentation capacity of NPC2$^{-/-}$ DCs directly isolated and purified from spleen and lymph nodes to understand these discrepancies.

With respect to lipid trafficking, cholesterol and gangliosides, including GM2 and GM3, have been shown to accumulate in mice deficient in NPC1 (27, 38). In addition, the transport of BODIPY-LacCer to the Golgi and of fluorescent αGalCer to the lysosome in NPC1$^{-/-}$ cells has been shown to be heavily perturbed with the presence of a late endosomal block (29, 37, 38). A similar study in NPC2$^{-/-}$ cells has been very limited besides establishing that some cell types were accumulating cholesterol in the absence of NPC2 (44). Moreover, important differences between NPC1$^{-/-}$ and NPC2$^{-/-}$ cells have been documented for the transport of GM2 ganglioside to the lysosome (45). Whereas NPC1$^{-/-}$ cells could not deliver GM2 to the lysosome, NPC2$^{-/-}$ cells could internalize GM2 into endocytic vesicles and deliver it to the lysosome (45). Our evaluation of the transport of LacCer and PBS-81 in NPC2$^{-/-}$ fibroblasts and splenocytes is very much in agreement with this observation. The transport of these two glycolipids through the endocytic pathway appeared close to normal in most cells. A morphometric quantification of these results will allow us to appreciate the precise numbers of vesicles in which lysosomal markers and PBS-81 colocalize in WT and mutant cells and also to compare the impact of NPC2 deficiency in different cell types. These major differences between NPC1$^{-/-}$ and NPC2$^{-/-}$ cells with respect to lipid endocytosis and transport reinforce the idea that the two molecules are present in different compartments: late endosomes for NPC1 and lysosomes for NPC2 (46, 47). This dichotomy could explain why NPC2 did not grossly perturb endocytosis and transport to the lysosome. However, the absence of NPC2 in the lysosome could affect the egress of lipids from this compartment; this issue will need further inquiry.

Our initial assessment of the degree of lipid storage in various cell types by using lysosomal dyes showed that NPC2 deficiency affected mostly splenocytes and BMDCs, whereas thymocytes were only marginally perturbed. We can conclude from this observation that lipid accumulation and presentation phenotypes are not correlated. This dissociation is one additional argument against a nonspecific effect of lipid storage as the cause for the observed phenotype resulting from the absence of NPC2.

Collectively, these observations suggest a direct role of NPC2 in the transport and loading of glycolipids into CD1d. The poor presentation of exogenous lipids and the almost complete absence of endogenous ligand presentation in NPC2$^{-/-}$ mice support this role, as does the in vitro loading of iGb3 into CD1d. However, the ability of recombinant NPC2 to complement the deficient phenotype is the most compelling argument supporting this hypothesis. In addition, the observation that only dimers of NPC2 are capable of transferring glycosphingolipids, whereas both dimers and monomers can bind cholesterol, suggests that the binding of cholesterol and the transfer of glycosphingolipids by NPC2 are mechanistically different. The engineering of mutants of NPC2, which cannot form dimers, will help clarify this point further.

In summary, this study establishes that NPC2 is critical for the loading of iGb3 and exogenous lipids into CD1d. This observation suggests a model in which multiple LTPs present in the CD1d-containing compartments, such as saposin and NPC2, select the repertoire of CD1d-presented lipids and glycosphingolipids (17, 18). The polymorphism of NPC2 will have to be studied in the context of NKT cells to determine whether pathological conditions are associated with variants of NPC2 that might affect immune functions.

MATERIALS AND METHODS

Mice. NPC2- and CD1d-deficient mice have been described previously (27, 48). NPC2 mice have been backcrossed six times in the BALB/c background. NPC2-deficient mice and littermate controls were obtained by intercrossing heterozygous mice. The genotype was determined by PCR as described previously (27). WT (NPC2$^{+/+}$) and heterozygote (NPC2$^{+/-}$) littermate mice were indistinguishable and are referred as WT. In all experiments, WT age-matched littermate mice were used as a control. NPC2-deficient mice are hypomorph, expressing 4–5% of the normal levels of NPC2. Genetrap NPC2-deficient mice in a BL6 background were also analyzed (B6;129P2-Npc2$^{Gt(pGT1TMpf5)1Ucd/Mmc}$; BayGenomics) and were indistinguishable from the hypomorph with respect to their immunological phenotype. All mice were bred at The Scripps Research Institute Animal Facility according to Institutional Animal Care and Use Committee guidelines.

Cell culture. Fresh thymocytes, splenocytes, liver lymphocytes, and cultured BMDCs were obtained as described previously (32, 35). Primary fibroblasts

were recovered from 7-d-old bone marrow culture by trypsination of the dish after washing out nonadherent cells. Cells were cultured in a 1:1 mixture of Click's medium and RPMI supplemented with 10% heat-inactivated FCS, glutamine, antibiotics, and 5×10^{-5} M β2- mercaptoethanol. Primary skin fibroblasts were obtained by digesting mice skin with 1 mg/ml collagenase D (Roche) at 37°C in DMEM supplemented with 10% heat-inactivated FCS for 5 h. After digestion, cells were washed several times in PBS and cultured in DMEM supplemented with 10% heat-inactivated FCS, glutamine, antibiotics, and 5×10^{-5} M β2-mercaptoethanol.

Flow cytometry. CD1d-αGalCer tetramers were generated and used as described previously (40). FITC-conjugated anti-CD4, –TCR-β, and - CD44 and allophycocyanin-conjugated anti-CD8 antibodies were purchased from BD Biosciences. Allophycocyanin-conjugated anti-B220 and -CD49b and PE–cyanin 7–conjugated anti-CD44 antibodies were obtained from eBioscience. Cells positive for propidium iodide and/or unloaded CD1d tetramer were excluded from analysis. Data were acquired using a flow cytometer (LSR2; Becton Dickinson) and analyzed using FACSDiva software (Becton Dickinson) and Flowjo software (Tree Star, Inc.). 10^6 events were typically recorded.

To evaluate lysosome size, thymocytes, splenocytes, BMDCs, and fibroblasts from 6-wk-old WT or NPC2$^{-/-}$ mice were stained with 200 nM Lysotracker green (Invitrogen) for 10 min. After washing, cells were analyzed by flow cytometry. Data were acquired using a FACSCalibur (Becton Dickinson) and Flowjo software. To evaluate cellular cholesterol content, cells from WT or NPC2$^{-/-}$ mice were fixed for 15 min with 4% paraformaldehyde, washed in Hanks' balanced salt solution, and stained for 2 h at 25°C with 100 μg/ml filipin (Sigma-Aldrich) in Hanks' balanced salt solution. Fluorescence emission was measured by flow cytometry (49).

T cell hybridoma in vitro stimulation. APCs used in T cell hybridoma in vitro stimulation were obtained from NPC2$^{-/-}$ and WT littermate mice between 3 and 9 wk of age. To measure autoreactivity, DN32.D3, TCB11, and TBD7 NKT hybridomas (5×10^4 cells/well) were incubated in the presence of 5×10^5 fresh thymocytes for 24 h, and IL-2 released in cultured supernatants was measured using an IL-2–dependent NK cell line (21). 0.5 μCi [^{3}H]thymidine was added to each well after a 24-h incubation. Results are expressed as mean counts per minute of triplicates.

To study the presentation of exogenous lipids, fresh thymocytes or splenocytes (5×10^4 cells/well) or 2×10^4 BMDCs were pulsed with or without NPC2 and various concentrations of lipids for 4 h. After incubation, APCs were washed three times and incubated with DN32.D3 hybridoma cells (5×10^4 cells/well) for 24 h. IL-2 released in cultured supernatants was measured as described in the previous paragraph.

To study the effect of recombinant NPC2 on autoreactivity, fresh thymocytes (5×10^4 cells/well) were incubated with or without NPC2 and DN32.D3 hybridoma cells (5×10^4 cells/well) for 24 h. IL-2 released in cultured supernatants was measured as described above.

To study MHC class II–mediated antigen presentation, after irradiation, splenocytes were incubated for 24 h with various concentrations of OVA protein and the T cell hybridoma specific for the peptide 323–339 of OVA in the context of I-A^d/I-A^b and DO11.10 (gift of S. Webb, The Scripps Research Institute, La Jolla, CA). IL-2 release in cultured supernatants was measured as described above. For whole spleen activation assay, fresh splenocytes (5×10^5 cells/well) were cultured with various concentrations of lipids for 48 h. IFN-γ released in the culture supernatant was measured by ELISA (BD Biosciences).

Mice immunization. WT or NPC2-deficient mice were immunized by i.v. injection in the tail vein with 2 μg αGalCer diluted in PBS or with vehicle only. Blood was collected at different time points after immunization and used for NKT cell analysis or IFN-γ production quantification.

Synthesis of Vα14 NKT cell ligands. PBS-81 was synthesized as reported previously for related compounds with the addition of the fluorophore (BODIPY FL; Invitrogen) at position six of the galactose via an amine (Fig. S8, available at http://www.jem.org/cgi/content/full/jem.20061562/DC1; reference 50). To incorporate the fluorophore, the *N*-hydroxylsuccinimicyl ester of 4,4-difluoro-5,7-dimethyl-4-bora-3a,4a-diaza-s-indacene-3-propionic acid (Invitrogen) was used. The structures of PBS-81 were confirmed by 1H and 13C nuclear magnetic resonance spectroscopy and mass spectrometry.

iGb3 C_8 and iGb3 C_{18} were synthesized as reported previously (Fig. S8; references 10, 29), and C8 and C18 acyl chains, respectively, were used in place of a C26 chain. The structures of iGb3 C_8 and IGb3 C_{18} were confirmed by 1H and 13C nuclear magnetic resonance spectroscopy and mass spectrometry.

Confocal microscopy. To study Vα14 NKT cell ligand trafficking, cells were grown on poly-L-lysine–coated coverslips (BD Biosciences) and incubated for 5 h or overnight with 10 μM PBS-81 at 37°C. To stain lysosomes, primary fibroblasts were incubated for 30 min with 1 μM Lysotracker red (Invitrogen), and splenocytes were incubated for 15 min with 0.1 μM Lysotracker red. For LacCer trafficking, cells were incubated for 30 min at 37°C with 5 μm BSA-complexed BODIPY FL C_5-LacCer (Invitrogen), washed three times with media, and incubated for 90 min at 37°C with media. Cells were washed three times with 2% FBS in PBS, and coverslips were mounted on slides with 2% FBS in PBS and a 1:50 dilution of oxyFluor (Oxyrase, Inc.). Live cells were examined immediately at room temperature by confocal microscopy using a laser-scanning confocal microscope (MRC1024; Bio-Rad Laboratories) with a 63× plan-Apo 1.4 NA oil objective lens (Carl Zeiss MicroImaging, Inc.) and a krypton/argon mixed gas laser, which excites at 488, 568, and 647 nm and records simultaneously in three separate channels.

To stain free cholesterol, cells were fixed with 4% paraformaldehyde for 15 min at 25°C, washed with PBS, and stained with 50 μg/ml filipin for 30 min. Cells were washed and analyzed with a laser-scanning confocal microscope (Radiance 2100 Rainbow; Bio-Rad Laboratories) with a 100× oil objective lens (Carl Zeiss MicroImaging, Inc.). For CD1d and Lamp-1 colocalization studies, after fixation with 3.7% formaldehyde for 15 min, cells were quenched for 10 min with 50 mM NH_4Cl in PBS and blocked with 4% FBS, 0.5% BSA, and 0.1% saponin in PBS for 30 min. Cells were incubated with a rat monoclonal anti-CD1d antibody (16G9; reference 51) in 4% FBS, 0.5% BSA, and 0.1% saponin in PBS for 60 min, washed with PBS, and incubated with a Texas red-X–conjugated goat anti–rat IgG antibody (Invitrogen). Cells were washed three times with PBS and incubated with a FITC-conjugated rat monoclonal anti–Lamp-1 antibody (BD Biosciences) in 4% FBS, 0.5% BSA, and 0.1% saponin in PBS for 60 min. Stained cells were mounted on slides with Mowiol (EMD Bioscience) and analyzed by confocal microscopy.

NPC2 and GM2a production/purification. Recombinant mouse NPC2 was expressed in a fly expression system (40). In brief, mouse NPC2 cDNA was subcloned into the expression vector pRMHa-3, and an N-terminal histidine tag was incorporated. Cells were cultured in roller bottles, and NPC2 protein was purified from the media using nickel-NTA agarose beads (QIAGEN) after tangential flow concentration. The protein was purified using a MonoS column (GE Healthcare) to further remove contaminating proteins and applied to a Superdex 200 column (GE Healthcare) to separate the dimer from the monomer form of NPC2. Fractions containing monomers only or enriched with the dimer forms of NPC2 were pooled and used for in vitro loading or activation assays. Mouse GM2a was produced using a similar approach and was purified by combination nickel-NTA agarose-ion exchange chromatography.

In vitro CD1d-loading assay. Recombinant mouse CD1d was expressed in a fly expression system (40). Purified complexes of CD1d–GT_{1b} were used to study the exchange of lipid into CD1d (21, 42). 2 μM mCD1d–GT_{1b} was incubated with various concentrations of NPC2 dimers and in the presence or absence of GM3 or iGb3. Lipid unloading and loading

into CD1d were visualized using IEF gel and were quantified using UN-SCAN-IT gel digitizing software (Silk Scientific; references 10, 21). The percentages were calculated as follows: percentage of GM3 loading into CD1d = (CD1d–GM3/(CD1d–GM3 + CD1d–GT)) × 100. Percentage of GT_{1b} unloading = (CD1d unloaded/(CD1d unloaded + CD1d–GT_{1b})) × 100.

RNA extraction and semiquantitative PCR. Fresh thymocytes and splenocytes from NPC2$^{-/-}$ and WT mice were obtained as previously described (32, 33). Cells were washed with cold PBS, and total RNA was isolated using TRIzol reagent (Invitrogen). cDNA were generated using 1 μg of total RNA and the Superscript III First-Strand synthesis system (Invitrogen). NPC2 and actin (used as an internal control) mRNA were amplified by PCR, and the products were visualized using agarose gel.

Expression of NPC2 in thymocytes. To test the expression of NPC2 in WT thymocytes and splenocytes, cells were washed with PBS and lysed by incubation for 30 min at room temperature in lysis buffer (60 mM Tris, pH 7.5, 150 mM NaCl, 2% SDS, and 1 U benzonase). Samples were resolved using 10–20% Tris-HCl precasted gels (Bio-Rad Laboratories). Proteins were electroblotted onto 0.2-μm polyvinylidene difluoride membranes, and membranes were blocked for 1 h with 10% FBS and 0.2% Triton X-100 in PBS. The membranes were then incubated for 1 h at room temperature with anti-NPC2 antibody (dilution of 1:250; polyclonal rabbit anti-NPC2 serum; gift from P. Lobel, Rutgers University, Piscataway, NJ). The blots were washed three times for 10 min with 0.2% Tween 20 in PBS and incubated for 1 h with peroxidase-labeled anti–rabbit immunoglobulin (dilution of 1:5,000; GE Healthcare). Blots were developed using SuperSignal (Pierce Chemical Co.).

Expression of NPC2 in HeLa cells. The mouse NPC2 cDNA was subcloned into the expression vector pcDNA3 with an N-terminal Flag tag. Cells were transiently transfected using LipofectAMINE (Invitrogen). 24 h after transfection, cells were washed with PBS and lysed by incubation for 30 min on ice with lysis buffer (50 mM Hepes, 100 mM NaCl, 10% glycerol, and 0.5% NP-40). Lysates were left untreated or were boiled for 5 min in the presence of 1% SDS and resolved using 10–20% Tris-HCl precasted gels. Proteins were detected by Western blotting using a monoclonal anti-Flag antibody (Sigma-Aldrich).

Cholesterol-binding assay. For binding measurements, NPC2 and DHE (Sigma-Aldrich) were diluted in PBS and incubated for 30 min at 25°C in the dark. 200-μl samples in quartz microcells were excited at 338 nm with a 0.5-nm bandpass slit. Emission spectra were obtained from 345 to 470 nm with a 4-nm bandpass slit. Fluorescence spectra were recorded by using a luminescence spectrometer (LS55; PerkinElmer).

Online supplemental material. Fig. S1 shows $CD4^+$ and $CD8^+$ T cells in the thymus and spleen and B cells in the spleen. Fig. S2 shows the thymic NKT cell phenotype in WT and NPC2$^{-/-}$ mice. Fig. S3 shows the expression of CD1d on thymocytes, splenocytes, and BMDCs from WT, NPC2$^{-/-}$, and CD1d$^{-/-}$ mice. Fig. S4 shows the expression of NPC2 in thymocytes and splenocytes. Fig. S5 shows cholesterol storage in WT and NPC2$^{-/-}$ cells. Fig. S6 shows the trafficking of a fluorescent-labeled derivative of αGalCer in WT and NPC2$^{-/-}$ primary skin fibroblasts. Fig. S7 shows that exogenous NPC2 protein enhances the presentation of αGalCer by splenocytes from WT and NPC2$^{-/-}$ mice. Fig. S8 shows a schematic representation of the structures of iGb3 C_8, iGb3 C_{18}, and PBS-81. Online supplemental material is available at http://www.jem.org/cgi/content/full/jem.20061562/DC1.

We thank P. Lobel for providing us with NPC2 mice (BALB/c and BayGenomics) and anti-NPC2 antibodies, Kenji Yoshida and Stefan Freigang for advice and discussion, and William B. Kiosses for help with confocal microscopy.

This work was supported by National Institutes of Health grant PO1AI053725 (to A. Bendelac, P.B. Savage, and L. Teyton) and grant AI038339 (to A. Bendelac) as well as a Cancer Research Institute Fellowship (to Y. Sagiv). A. Bendelac is a Howard Hughes Medical Institute Investigator.

The authors have no conflicting financial interests.

Submitted: 25 July 2006
Accepted: 28 February 2007

REFERENCES

1. Calabi, F., J.M. Jarvis, L. Martin, and C. Milstein. 1989. Two classes of CD1 genes. *Eur. J. Immunol.* 19:285–292.
2. Porcelli, S.A., and R.L. Modlin. 1999. The CD1 system: antigen-presenting molecules for T cell recognition of lipids and glycolipids. *Annu. Rev. Immunol.* 17:297–329.
3. Brossay, L., D. Jullien, S. Cardell, B.C. Sydora, N. Burdin, R.L. Modlin, and M. Kronenberg. 1997. Mouse CD1 is mainly expressed on hemopoietic-derived cells. *J. Immunol.* 159:1216–1224.
4. Mandal, M., X.R. Chen, M.L. Alegre, N.M. Chiu, Y.H. Chen, A.R. Castano, and C.R. Wang. 1998. Tissue distribution, regulation and intracellular localization of murine CD1 molecules. *Mol. Immunol.* 35:525–536.
5. Jahng, A., I. Maricic, C. Aguilera, S. Cardell, R.C. Halder, and V. Kumar. 2004. Prevention of autoimmunity by targeting a distinct, non-invariant CD1d-reactive T cell population reactive to sulfatide. *J. Exp. Med.* 199:947–957.
6. Zajonc, D.M., I. Maricic, D. Wu, R. Halder, K. Roy, C.H. Wong, V. Kumar, and I.A. Wilson. 2005. Structural basis for CD1d presentation of a sulfatide derived from myelin and its implications for autoimmunity. *J. Exp. Med.* 202:1517–1526.
7. Fischer, K., E. Scotet, M. Niemeyer, H. Koebernick, J. Zerrahn, S. Maillet, R. Hurwitz, M. Kursar, M. Bonneville, S.H. Kaufmann, and U.E. Schaible. 2004. Mycobacterial phosphatidylinositol mannoside is a natural antigen for CD1d-restricted T cells. *Proc. Natl. Acad. Sci. USA.* 101:10685–10690.
8. MacDonald, H.R. 2002. Development and selection of NKT cells. *Curr. Opin. Immunol.* 14:250–254.
9. Kawano, T., J. Cui, Y. Koezuka, I. Toura, Y. Kaneko, K. Motoki, H. Ueno, R. Nakagawa, H. Sato, E. Kondo, et al. 1997. CD1d-restricted and TCR-mediated activation of valpha14 NKT cells by glycosylceramides. *Science.* 278:1626–1629.
10. Zhou, D., J. Mattner, C. Cantu III, N. Schrantz, N. Yin, Y. Gao, Y. Sagiv, K. Hudspeth, Y.P. Wu, T. Yamashita, et al. 2004. Lysosomal glycosphingolipid recognition by NKT cells. *Science.* 306:1786–1789.
11. Godfrey, D.I., H.R. MacDonald, M. Kronenberg, M.J. Smyth, and L. Van Kaer. 2004. NKT cells: what's in a name? *Nat. Rev. Immunol.* 4:231–237.
12. Bendelac, A., M.N. Rivera, S.H. Park, and J.H. Roark. 1997. Mouse CD1-specific NK1 T cells: development, specificity, and function. *Annu. Rev. Immunol.* 15:535–562.
13. Wei, D.G., H. Lee, S.H. Park, L. Beaudoin, L. Teyton, A. Lehuen, and A. Bendelac. 2005. Expansion and long-range differentiation of the NKT cell lineage in mice expressing CD1d exclusively on cortical thymocytes. *J. Exp. Med.* 202:239–248.
14. Jayawardena-Wolf, J., K. Benlagha, Y.H. Chiu, R. Mehr, and A. Bendelac. 2001. CD1d endosomal trafficking is independently regulated by an intrinsic CD1d-encoded tyrosine motif and by the invariant chain. *Immunity.* 15:897–908.
15. Conzelmann, E., and K. Sandhoff. 1980. The specificity of human N-acetyl-beta-D-hexosaminidases towards glycosphincolipids is determined by an activator protein. *Adv. Exp. Med. Biol.* 125:295–306.
16. Sandhoff, K., and T. Kolter. 1998. Processing of sphingolipid activator proteins and the topology of lysosomal digestion. *Acta Biochim. Pol.* 45:373–384.
17. Sleat, D.E., H. Lackland, Y. Wang, I. Sohar, G. Xiao, H. Li, and P. Lobel. 2005. The human brain mannose 6-phosphate glycoproteome: a complex mixture composed of multiple isoforms of many soluble lysosomal proteins. *Proteomics.* 5:1520–1532.
18. Kollmann, K., K.E. Mutenda, M. Balleininger, E. Eckermann, K. von Figura, B. Schmidt, and T. Lubke. 2005. Identification of novel lysosomal matrix proteins by proteome analysis. *Proteomics.* 5:3966–3978.

19. Hiraiwa, M., S. Soeda, Y. Kishimoto, and J.S. O'Brien. 1992. Binding and transport of gangliosides by prosaposin. *Proc. Natl. Acad. Sci. USA*. 89:11254–11258.
20. Hama, Y., Y.T. Li, and S.C. Li. 1997. Interaction of GM2 activator protein with glycosphingolipids. *J. Biol. Chem*. 272:2828–2833.
21. Zhou, D., C. Cantu III, Y. Sagiv, N. Schrantz, A.B. Kulkarni, X. Qi, D.J. Mahuran, C.R. Morales, G.A. Grabowski, K. Benlagha, et al. 2004. Editing of CD1d-bound lipid antigens by endosomal lipid transfer proteins. *Science*. 303:523–527.
22. Naureckiene, S., D.E. Sleat, H. Lackland, A. Fensom, M.T. Vanier, R. Wattiaux, M. Jadot, and P. Lobel. 2000. Identification of HE1 as the second gene of Niemann-Pick C disease. *Science*. 290:2298–2301.
23. Willenborg, M., C.K. Schmidt, P. Braun, J. Landgrebe, K. von Figura, P. Saftig, and E.L. Eskelinen. 2005. Mannose 6-phosphate receptors, Niemann-Pick C2 protein, and lysosomal cholesterol accumulation. *J. Lipid Res*. 46:2559–2569.
24. Cheruku, S.R., Z. Xu, R. Dutia, P. Lobel, and J. Storch. 2006. Mechanism of cholesterol transfer from the Niemann-Pick type C2 protein to model membranes supports a role in lysosomal cholesterol transport. *J. Biol. Chem*. 281:31594–31604.
25. Vanier, M.T., S. Duthel, C. Rodriguez-Lafrasse, P. Pentchev, and E.D. Carstea. 1996. Genetic heterogeneity in Niemann-Pick C disease: a study using somatic cell hybridization and linkage analysis. *Am. J. Hum. Genet*. 58:118–125.
26. Steinberg, S.J., C.P. Ward, and A.H. Fensom. 1994. Complementation studies in Niemann-Pick disease type C indicate the existence of a second group. *J. Med. Genet*. 31:317–320.
27. Sleat, D.E., J.A. Wiseman, M. El-Banna, S.M. Price, L. Verot, M.M. Shen, G.S. Tint, M.T. Vanier, S.U. Walkley, and P. Lobel. 2004. Genetic evidence for nonredundant functional cooperativity between NPC1 and NPC2 in lipid transport. *Proc. Natl. Acad. Sci. USA*. 101:5886–5891.
28. Vanier, M.T., and G. Millat. 2004. Structure and function of the NPC2 protein. *Biochim. Biophys. Acta*. 1685:14–21.
29. Sagiv, Y., K. Hudspeth, J. Mattner, N. Schrantz, R.K. Stern, D. Zhou, P.B. Savage, L. Teyton, and A. Bendelac. 2006. Cutting edge: impaired glycosphingolipid trafficking and NKT cell development in mice lacking Niemann-Pick type c1 protein. *J. Immunol*. 177:26–30.
30. Stenstrom, M., M. Skold, A. Andersson, and S.L. Cardell. 2005. Natural killer T-cell populations in C57BL/6 and NK1.1 congenic BALB.NK mice-a novel thymic subset defined in BALB.NK mice. *Immunology*. 114:336–345.
31. Berzins, S.P., F.W. McNab, C.M. Jones, M.J. Smyth, and D.I. Godfrey. 2006. Long-term retention of mature NK1.1+ NKT cells in the thymus. *J. Immunol*. 176:4059–4065.
32. Chiu, Y.H., J. Jayawardena, A. Weiss, D. Lee, S.H. Park, A. Dautry-Varsat, and A. Bendelac. 1999. Distinct subsets of CD1d-restricted T cells recognize self-antigens loaded in different cellular compartments. *J. Exp. Med*. 189:103–110.
33. Prigozy, T.I., O. Naidenko, P. Qasba, D. Elewaut, L. Brossay, A. Khurana, T. Natori, Y. Koezuka, A. Kulkarni, and M. Kronenberg. 2001. Glycolipid antigen processing for presentation by CD1d molecules. *Science*. 291:664–667.
34. Carnaud, C., D. Lee, O. Donnars, S.H. Park, A. Beavis, Y. Koezuka, and A. Bendelac. 1999. Cutting edge: cross-talk between cells of the innate immune system: NKT cells rapidly activate NK cells. *J. Immunol*. 163:4647–4650.
35. Chiu, Y.H., S.H. Park, K. Benlagha, C. Forestier, J. Jayawardena-Wolf, P.B. Savage, L. Teyton, and A. Bendelac. 2002. Multiple defects in antigen presentation and T cell development by mice expressing cytoplasmic tail-truncated CD1d. *Nat. Immunol*. 3:55–60.
36. Liscum, L., and J.R. Faust. 1989. The intracellular transport of low density lipoprotein-derived cholesterol is inhibited in Chinese hamster ovary cells cultured with 3-beta-[2-(diethylamino)ethoxy]androst-5-en-17-one. *J. Biol. Chem*. 264:11796–11806.
37. Pentchev, P.G., M.E. Comly, H.S. Kruth, M.T. Vanier, D.A. Wenger, S. Patel, and R.O. Brady. 1985. A defect in cholesterol esterification in Niemann-Pick disease (type C) patients. *Proc. Natl. Acad. Sci. USA*. 82:8247–8251.
38. Narita, K., A. Choudhury, K. Dobrenis, D.K. Sharma, E.L. Holicky, D.L. Marks, S.U. Walkley, and R.E. Pagano. 2005. Protein transduction of Rab9 in Niemann-Pick C cells reduces cholesterol storage. *FASEB J*. 19:1558–1560.
39. Gadola, S.D., J.D. Silk, A. Jeans, P.A. Illarionov, M. Salio, G.S. Besra, R. Dwek, T.D. Butters, F.M. Platt, and V. Cerundolo. 2006. Impaired selection of invariant natural killer T cells in diverse mouse models of glycosphingolipid lysosomal storage diseases. *J. Exp. Med*. 203:2293–2303.
40. Benlagha, K., A. Weiss, A. Beavis, L. Teyton, and A. Bendelac. 2000. In vivo identification of glycolipid antigen-specific T cells using fluorescent CD1d tetramers. *J. Exp. Med*. 191:1895–1903.
41. Friedland, N., H.L. Liou, P. Lobel, and A.M. Stock. 2003. Structure of a cholesterol-binding protein deficient in Niemann-Pick type C2 disease. *Proc. Natl. Acad. Sci. USA*. 100:2512–2517.
42. Cantu, C., III, K. Benlagha, P.B. Savage, A. Bendelac, and L. Teyton. 2003. The paradox of immune molecular recognition of alpha-galactosylceramide: low affinity, low specificity for CD1d, high affinity for alpha beta TCRs. *J. Immunol*. 170:4673–4682.
43. Fujii, S., K. Shimizu, M. Kronenberg, and R.M. Steinman. 2002. Prolonged IFN-gamma-producing NKT response induced with alpha-galactosylceramide-loaded DCs. *Nat. Immunol*. 3:867–874.
44. Blom, T.S., M.D. Linder, K. Snow, H. Pihko, M.W. Hess, E. Jokitalo, V. Veckman, A.C. Syvanen, and E. Ikonen. 2003. Defective endocytic trafficking of NPC1 and NPC2 underlying infantile Niemann-Pick type C disease. *Hum. Mol. Genet*. 12:257–272.
45. Zhang, M., M. Sun, N.K. Dwyer, M.E. Comly, S.C. Patel, R. Sundaram, J.A. Hanover, and E.J. Blanchette-Mackie. 2003. Differential trafficking of the Niemann-Pick C1 and 2 proteins highlights distinct roles in late endocytic lipid trafficking. *Acta Paediatr. Suppl*. 92:63–73.
46. Neufeld, E.B., M. Wastney, S. Patel, S. Suresh, A.M. Cooney, N.K. Dwyer, C.F. Roff, K. Ohno, J.A. Morris, E.D. Carstea, et al. 1999. The Niemann-Pick C1 protein resides in a vesicular compartment linked to retrograde transport of multiple lysosomal cargo. *J. Biol. Chem*. 274:9627–9635.
47. Zhang, M., N.K. Dwyer, D.C. Love, A. Cooney, M. Comly, E. Neufeld, P.G. Pentchev, E.J. Blanchette-Mackie, and J.A. Hanover. 2001. Cessation of rapid late endosomal tubulovesicular trafficking in Niemann-Pick type C1 disease. *Proc. Natl. Acad. Sci. USA*. 98:4466–4471.
48. Park, S.H., D. Guy-Grand, F.A. Lemonnier, C.R. Wang, A. Bendelac, and B. Jabri. 1999. Selection and expansion of CD8alpha/alpha(1) T cell receptor alpha/beta(1) intestinal intraepithelial lymphocytes in the absence of both classical major histocompatibility complex class I and nonclassical CD1 molecules. *J. Exp. Med*. 190:885–890.
49. Muller, C.P., D.A. Stephany, D.F. Winkler, J.M. Hoeg, S.J. Demosky Jr., and J.R. Wunderlich. 1984. Filipin as a flow microfluorometry probe for cellular cholesterol. *Cytometry*. 5:42–54.
50. Zhou, X.T., C. Forestier, R.D. Goff, C. Li, L. Teyton, A. Bendelac, and P.B. Savage. 2002. Synthesis and NKT cell stimulating properties of fluorophore- and biotin-appended 6"-amino-6"-deoxy-galactosylceramides. *Org. Lett*. 4:1267–1270.
51. Roark, J.H., S.H. Park, J. Jayawardena, U. Kavita, M. Shannon, and A. Bendelac. 1998. CD1.1 expression by mouse antigen-presenting cells and marginal zone B cells. *J. Immunol*. 160:3121–3127.